

BBABIO 43435

## Kinetic study of the aspartate/glutamate carrier in intact rat heart mitochondria and comparison with a reconstituted system

Francis E. Sluse<sup>1</sup>, Alain Evens<sup>1</sup>, Thomas Dierks<sup>2</sup>, Claire Duyckaerts<sup>1</sup>,  
Claudine M. Sluse-Goffart<sup>1</sup> and Reinhard Krämer<sup>2</sup>

<sup>1</sup> Laboratoire de Bioénergétique, Institut de Chimie, Sart-Tilman, Université de Liège, (Belgium) and <sup>2</sup> Institut für Biotechnologie 1, Forschungszentrum Jülich, Jülich (F.R.G.)

(Received 7 September 1990)

(Revised manuscript received 22 February 1991)

Key words: Mitochondrion; Aspartate/glutamate carrier; Kinetic mechanism; Reconstitution; Transmembrane orientation; Carrier-mediated transport

The homologous exchange of external [<sup>14</sup>C]aspartate/internal aspartate catalyzed by the aspartate/glutamate carrier of rat heart mitochondria was investigated using aspartate-loaded, glutamate-depleted mitochondria. An inhibitor-stop technique was developed for kinetic studies by applying pyridoxal phosphate. Direct initial rate determinations from the linear phase of [<sup>14</sup>C]aspartate uptake were insufficiently accurate at high external and/or low internal substrate concentrations. Therefore, the full time-course of [<sup>14</sup>C]aspartate uptake until reaching isotope equilibrium was fitted by a single exponential function and was used to calculate reliable initial steady-state rates. This method was applied in bisubstrate analyses of the antiport reaction for different external and internal aspartate concentrations. The kinetic patterns obtained in double reciprocal plots showed straight lines converging on the abscissa. This result is consistent with a sequential antiport mechanism. It implies the existence of a catalytic ternary complex that is formed by the translocator and substrate molecules bound from both sides of the membrane. The  $K_m$  values for aspartate were clearly different for the external and the internal sides of the membrane,  $216 \pm 23 \mu\text{M}$  and  $2.4 \pm 0.5 \text{ mM}$ , respectively. These values indicated a definite transmembrane asymmetry of the carrier. The same asymmetry became evident when investigating the isolated protein from bovine heart mitochondria after reconstitution into liposomes. In this case the  $K_m$  values for external and internal aspartate were determined to be  $123 \pm 11 \mu\text{M}$  and  $2.8 \pm 0.6 \text{ mM}$ , respectively. This comparison demonstrates a right-side out orientation of the carrier after insertion into liposomal membranes. The sequential transport mechanism of the aspartate/glutamate carrier, elucidated both in proteoliposomes and in mitochondria, also seems to be a common characteristic of other mitochondrial antiport carriers.

### Introduction

The molecular mechanism of any biomembrane carrier is far from being elucidated from structure-function relationships because the structural information available cannot be unequivocally interpreted in terms of transport mechanism. Therefore, information about carrier function obtained by kinetics, the most powerful approach to discriminate between mechanisms, imposes strict limitations on the interpretation of structural and molecular data.

Few of the specific carriers catalyzing antiport processes in the inner mitochondrial membrane have been extensively investigated in order to determine their mechanism in kinetic terms. The first antiporter to be carefully studied as a classic bireactant system was the oxoglutarate carrier of rat heart mitochondria. It was investigated via bisubstrate analyses of initial rates [1] as well as substrate competition experiments [2]. The results led to the conclusion that the oxoglutarate carrier follows a sequential mechanism involving a ternary complex of the protein and two substrate ligands. This catalytic complex is formed by rapid-equilibrium random binding of substrate molecules to an independent internal and external binding site. Moreover, detailed kinetic studies have shown that the be-

Correspondence: F. Sluse, Unité de Bioénergétique, Université de Liège, Institut de Chimie (B-6) Sart-Tilman, B-4000 Liège, Belgium.

haviour of the translocator is intrinsically asymmetric regarding the two sides of the membrane and the two exchanged substrates, oxoglutarate and malate (for review see Ref. 3 and 4).

Further attempts at classic kinetic studies in mitochondria were undertaken on the aspartate/glutamate carrier [5,6] and on the ADP/ATP carrier [7–9]. These studies led to fundamental contradictions in the conclusions drawn by different groups. Mainly technical problems impeded initial rate measurements in intact mitochondria at various concentrations of both external and internal substrate. A set of prerequisites must be fulfilled for initial rate analysis under these conditions (as discussed in Ref. 9).

Another way to elucidate catalytic mechanisms of carriers which avoids several methodological difficulties, is to establish a well-defined reconstituted system and to use it for kinetic studies, provided the carrier is not randomly oriented in the liposomal membrane. The kinetic mechanism of the aspartate/glutamate carrier was successfully determined [10] for such a system [11–13] and was demonstrated to be the same type of sequential mechanism as described for the oxoglutarate carrier. The substrate affinities were clearly different for the two different membrane sides for both aspartate and glutamate. When the affinity constants were compared with published data obtained in mitochondria and submitochondrial particles [5,6] an inside out orientation of the carrier protein in the liposomes was suggested [13].

The controversy surrounding the results, obtained for the antiport mechanism of the aspartate/glutamate carrier and its transport affinity constants in mitochondria, emphasizes the need to revisit this carrier. In the present paper these problems have been addressed on the basis of experiments using both intact mitochondria and a reconstituted system which led to concordant results. Part of these results has been presented briefly elsewhere [14–16].

## Material and Methods

### *Preparation and loading of mitochondria*

Rats were 200–250 g fed males from Wistar strain. Mitochondria from heart ventricles were prepared according to Tyler and Gonze [17], the isolation medium contained 225 mM mannitol, 75 mM sucrose and 0.05 mM EDTA neutralized with 1 mM Tris. These crude mitochondria contained approx. 6 mM aspartate and 2.5 mM glutamate. The study of the homoexchange  $\text{aspartate}_{\text{out}}/\text{aspartate}_{\text{in}}$  required glutamate-depleted, aspartate-loaded mitochondria with different levels of aspartate:

(a) The internal level of glutamate was reduced by a 30-min incubation at 0°C in isolation medium containing 20 mM Tris-HCl buffer (pH 7.4) and 5 mM malate (Mal-incubation). The matricial oxaloacetate produced by oxidation of the entered malate was transaminated by glutamate leading to aspartate and oxoglutarate, the latter being metabolized. The Mal-incubation provided a mitochondrial preparation with a high internal aspartate concentration and a low level of glutamate (Table I, line 1). The presence of internal malate (3–6 mM) does not interfere with this, since neither malate nor oxoglutarate influence the activity of the purified aspartate/glutamate carrier reincorporated into proteoliposomes (Dierks, T., unpublished data);

(b) A mitochondrial preparation containing a medium level of aspartate was obtained by performing a 30-min incubation in isolation medium containing 20 mM Tris-HCl (pH 7.4), 5 mM oxoglutarate and 1 mM arsenite (OG-incubation) before the Mal-incubation. The displacement of the equilibrium of the reaction catalyzed by the glutamate-oxaloacetate transaminase by oxoglutarate transformed aspartate to oxaloacetate and finally to malate. There was a parallel increase of glutamate released into the incubation medium via the glutamate/ $\text{OH}^-$  carrier. The OG-incubation reduced the total pool of aspartate plus glutamate. The ensuing

TABLE 1

### *Loading of mitochondria*

Aspartate and glutamate concentrations of the mitochondrial matrix as determined after different incubations of mitochondria (see Materials and Methods). D.M., depletion medium; (6–8), number of measurements.

	Incubations				Aspartate (mM)	Glutamate (mM)
	OG	Mal	D.M.	Asp		
1	–	+	–	–	5.0	0.29
2	+	+	–	–	2.6	0.62
3	–	+	+	–	0.18	0.13
4	–	+	–	+	5.0 ± 1.2 (7)	0.36 ± 0.08 (7)
5	+	+	–	+	3.3 ± 1.0 (8)	0.18 ± 0.07 (8)
6	–	+	+	+	0.98 ± 0.34 (7)	0.07 ± 0.01 (6)

Mal-incubation decreased (as in (a)) the internal level of glutamate with a parallel increase in aspartate (Table I, line 2); and

(c) A low internal aspartate concentration was achieved by a 10-min incubation at 25°C of the mitochondrial preparation obtained in (a) in the medium usually applied to obtain malate-depleted mitochondria (depletion medium) [18] leading to a concomitant decrease of aspartate (Table I, line 3).

In order to improve the glutamate depletion by an exchange  $\text{aspartate}_{\text{out}}/(\text{glutamate-H}^+)_{\text{in}}$ , the three mitochondrial preparations were incubated for 30 min at 0°C in isolation medium containing 20 mM Tris-HCl (pH 7.4) and 10 mM aspartate (Asp-incubation). During this step 2 mM aminooxyacetate, an inhibitor of transaminases but not of the aspartate/glutamate carrier as tested in the reconstituted system, was present. Under these conditions the glutamate level in preparations (b) and (c) decreased and did not exceed 8% of the internal aspartate level for the high, medium or low concentrations (Table I, lines 4–6).

All mitochondrial preparations were finally washed in a large volume of the isolation medium (containing 2 mM aminooxyacetate) to eliminate external aspartate contamination and resuspended in a small volume of the medium (10 mg mitochondrial protein/ml).

The aspartate and glutamate content of the mitochondrial matrix was determined after perchlorate extraction of sedimented mitochondria. An aliquot (1  $\mu\text{l}$ ) of the extract supernatant, after neutralization with carbonate/KOH, was applied to a reversed-phase column (Merck Licrospher RP-18, 150  $\times$  3 mm). Separation of amino acids was carried out according to the method of Jones and Gilligan [19] using a gradient HPLC system (HP 1090M, Hewlett Packard). The amino acids were detected fluorometrically after pre-column derivatization with *o*-phthalaldehyde. Internal concentrations could be calculated on the basis of matrix volumes, which were determined from the [ $^3\text{H}$ ]water content of the mitochondrial pellet taking into account the [ $^{14}\text{C}$ ]sucrose-accessible space [20].

#### *Kinetic measurements with mitochondria: improvement of incubation conditions and stop-technique*

The stock suspension of glutamate-depleted and aspartate-loaded mitochondria (0.5 mg protein) was diluted in incubation medium which contained 22.5 mM mannitol, 7.5 mM sucrose, 15 mM KCl, 5 mM  $\text{MgCl}_2$ , 2 mM EDTA and 50 mM Tris-HCl (pH 7.4). Aspartate/aspartate exchange was measured at 2°C by following the uptake of [ $^{14}\text{C}$ ]aspartate. The inhibitor-stop technique applied was as described previously [18] but using pyridoxal phosphate as inhibitor (see below). Labelled aspartate dissolved in the incubation medium and inhibitor were added with Hamilton syringes (CR-700) allowing instantaneous mixing.

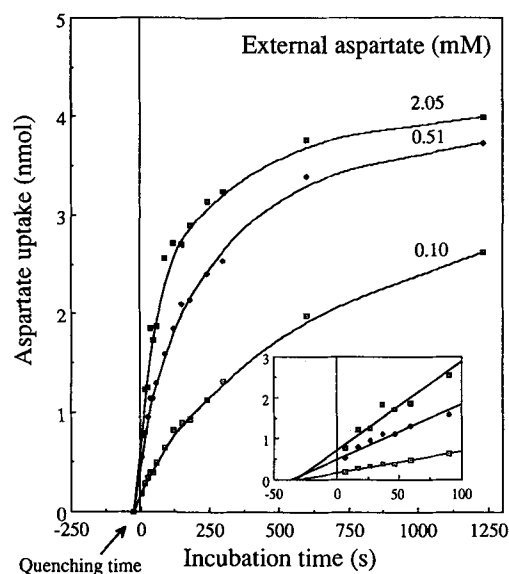


Fig. 1. Time-course of [ $^{14}\text{C}$ ]aspartate $_{\text{out}}$ /aspartate $_{\text{in}}$  exchange in aspartate-loaded, glutamate-unloaded mitochondria (centrifugation-stop). The exchange was started by injection of [ $^{14}\text{C}$ ]aspartate and stopped by centrifugation (2.5  $\mu\text{l}$  mitochondrial pellet corresponding to 0.5 mg protein). The [ $^{14}\text{C}$ ]aspartate in the mitochondrial pellet was corrected for contamination in the sucrose-accessible space. [Asp] $_{\text{in}}$  = 4.8 mM (5 nmol), [Glu] $_{\text{in}}$  = 0.13 mM.

In a first attempt, the time-course was followed for [ $^{14}\text{C}$ ]aspartate uptake up to 30 min using a rapid centrifugation-stop technique. The transport was measured at 2°C in the presence of 2 mM aminooxyacetate, an inhibitor of glutamate-oxaloacetate transaminase, both in the stock suspension of mitochondria and in the incubation medium. The internal aspartate concentration was 3.25 mM and three external [ $^{14}\text{C}$ ]aspartate concentrations were tested between 0.02 and 1.8 mM. Under these conditions the uptake of labelled aspartate exceeded the theoretical value of isotope equilibration which can be calculated on the basis of the amount of unlabelled aspartate available inside the matrix (not shown). This observation suggested a rapid metabolism of the substrate which entered and an accumulation of radioactive metabolites in the matrix.

If the same time-course was recorded in the presence of aminooxyacetate with, additionally, 2 mM cycloserine, rotenone (4  $\mu\text{g}/\text{mg}$  protein) and antimycin (6  $\mu\text{g}/\text{mg}$  protein), the uptake of labelled aspartate remained lower than the available internal aspartate (5 nmol) for all three external substrate concentrations tested, as shown in Fig. 1. This means that [ $^{14}\text{C}$ ]aspartate taken up was not metabolized under these conditions. The equilibrium was approached at incubation times higher than 30 min (not shown). The inset of Fig. 1, magnifying the initial phase, shows that the quenching (sedimentation) time was not negligible compared with the linear part of the time-course. These observa-

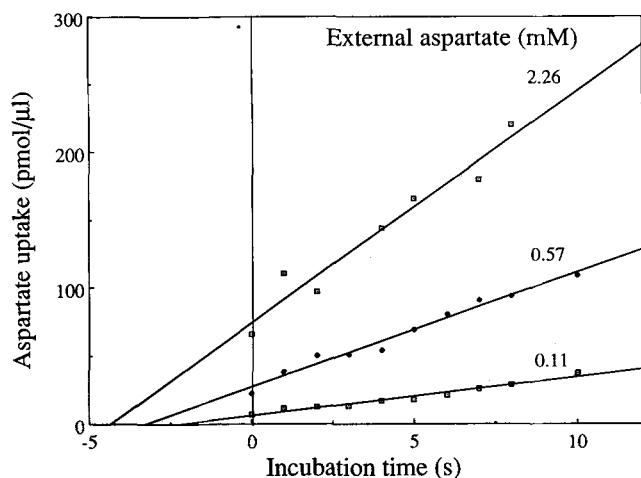


Fig. 2. Inhibitor-stop measurement of [ $^{14}\text{C}$ ]aspartate uptake by aspartate-loaded mitochondria. Incubation time represents the interval between the injections of labelled aspartate and inhibitor (23 mM pyridoxal phosphate);  $[\text{Asp}]_{\text{in}} = 5.8 \text{ mM}$ ,  $[\text{Glu}]_{\text{in}} = 0.30 \text{ mM}$ . The uptake was corrected for the amount of [ $^{14}\text{C}$ ]aspartate accumulated in the mitochondrial pellet when the inhibitor was injected 5 s before the substrate and is given in  $\text{pmol}/\mu\text{l}$  of mitochondrial pellet.

tions led to two conclusions: (a) the matricial metabolism of aspartate can be frozen by the inhibitor cocktail, and (b) the exchange had to be blocked by an inhibitor-stop technique in order to reduce the quenching time.

Pyridoxal phosphate was used for this purpose. It has been described as an effective, though unspecific inhibitor of reconstituted aspartate/glutamate transport [13] acting on the cytosolic surface of the protein (unpublished data). When the inhibitor was added 5 s before [ $^{14}\text{C}$ ]aspartate, the radioactivity in the mitochondrial pellet was equal to that of the aspartate in the sucrose-accessible space indicating a complete block of the substrate uptake. Thus, the amount of [ $^{14}\text{C}$ ]aspartate in the pellet, determined when the inhibitor was added 5 s before the labelled substrate, was subtracted from all other values. Fig. 2 shows the data, corrected accordingly, for the first 10 s of uptake (0.11, 0.57 and 2.26 mM [ $^{14}\text{C}$ ]aspartate). A linear phase of uptake (about 10 s) existed even at high external substrate concentrations. The intercepts on the ordinate indicate that the uptake was not zero when inhibitor and substrate were added simultaneously; however, the observed quench delay was shorter than 5 s even at the highest external aspartate concentration. After this delay the inhibition was complete, since no additional uptake was measured. The initial rates are properly determined despite the quench delay because this delay is much lower than the characteristic time of relaxation towards equilibrium (134, 270 and 741 s at 2.26, 0.57 and 0.11 mM external aspartate, respectively).

### Kinetic analysis of the reconstituted aspartate / glutamate carrier

The isolation of the aspartate/glutamate carrier from bovine heart mitochondria and its functional reconstitution was described in [11–13]. The reconstituted transport activity was determined at room temperature by the forward exchange method measuring uptake of labelled aspartate into the proteoliposomes [13]. The time-course (first 4 min) of the isotope equilibration was fitted by a first-order rate equation using a computer program that enabled initial rates of transport to be derived [21].

The dependence of the transport affinity of the reconstituted carrier for external and internal aspartate on pH was determined by varying the pH simultaneously inside and outside the proteoliposomes ( $\Delta \text{pH} = 0$ ). The pH was adjusted by passing three aliquots of proteoliposomes, prepared at pH 6.9 (100 mM Mops/KOH) and supplemented with valinomycin (700 ng/mg phospholipid) and nigericin (40 ng/mg phospholipid), through Sephadex G-75 columns which were equilibrated with 100 mM Mops/KOH at pH 6.5, 6.9 or 7.4. This buffer contained sucrose to balance the osmolarity of the internal aspartate.

### Chemicals

Special reagents were obtained from the following sources: [ $\text{U-}^{14}\text{C}$ ]aspartic acid, [ $\text{U-}^{14}\text{C}$ ]sucrose and  $^3\text{H}_2\text{O}$  (Amersham); rotenone, aminooxyacetate and cycloserine (Sigma); antimycin (Boehringer Mannheim) and pyridoxal phosphate (Merck).

### Results

In order to study the antiport activity of the aspartate/glutamate carrier in intact mitochondria the kinetic experiments had to be made as clear-cut as possible. To choose the simplest conditions, the electroneutral homologous exchange [ $^{14}\text{C}$ ]aspartate<sub>out</sub>/aspartate<sub>in</sub> was investigated. By using aspartate-loaded and glutamate-depleted mitochondria no significant net-import of aspartate from the incubation medium (in exchange for matricial glutamate) could take place, thus avoiding changes of substrate concentrations during the transport assay. The metabolism of aspartate could efficiently be blocked by working at 2°C and by applying several inhibitors of transamination and respiration (see Materials and Methods).

### Initial rate measurements

The activity of aspartate/aspartate exchange was investigated at various internal and external substrate concentrations using the inhibitor-stop technique described in Materials and Methods. Initial rates could be evaluated directly from the slope of the first linear phase of [ $^{14}\text{C}$ ]aspartate uptake. Such initial conditions,

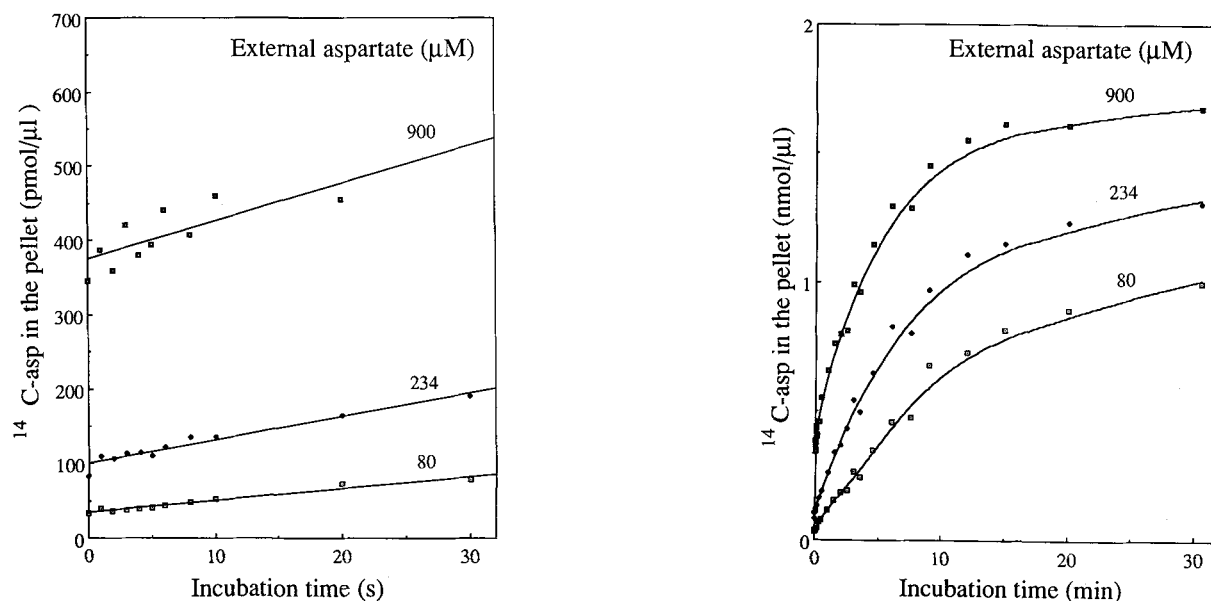


Fig. 3. Initial rates and full progress-curves of  $[^{14}\text{C}]\text{aspartate}_{\text{out}}/\text{aspartate}_{\text{in}}$  exchange. (A) Initial rates of the  $[^{14}\text{C}]\text{aspartate}_{\text{out}}/\text{aspartate}_{\text{in}}$  exchange;  $[\text{Asp}]_{\text{in}} = 4.92 \text{ mM}$ ,  $[\text{Glu}]_{\text{in}} = 0.47 \text{ mM}$ . The aspartate uptake for incubation time = 0 (simultaneous injection of aspartate and 23 mM pyridoxal phosphate) corresponds to the residual uptake after the injection of the inhibitor plus the aspartate content in the sucrose accessible space (not corrected). (B) Same experiment as in (A), data shown for longer incubation times (full progress-curve).

however, occurred only for a short time at high external aspartate concentrations. This is illustrated in Fig. 3, where the  $[^{14}\text{C}]\text{aspartate}$  content of sedimented mitochondria was plotted vs. time, as recorded for three external aspartate concentrations (80, 234 and  $900 \mu\text{M}$ ) at constant internal aspartate ( $4.9 \text{ mM}$ ). The initial phase (Fig. 3A) revealed that linearity lasted for 20–30 s. Within this period the amount of isotope exchanged was less than 6% for the internal substrate and negligible ( $< 1\%$ ) for the external substrate. The slopes of the straight lines can thus be considered as initial rates of the exchange amounting to  $1.61 \pm 0.11$ ,  $3.16 \pm 0.27$  and  $5.11 \pm 1.53 \text{ pmol/s per } \mu\text{l}$  of mitochondrial pellet for 80, 234 and  $900 \mu\text{M}$  external aspartate, respectively. It became obvious, however, that the accuracy of the slopes was unsatisfactory and that the error increased with the external substrate concentration. This was due to the fact that the signal to be detected, namely the uptake of  $[^{14}\text{C}]\text{aspartate}$  into the matrix, is only part of the overall radioactivity in the mitochondrial pellet and this part decreased when the external concentration was increased. At  $900 \mu\text{M}$  external aspartate the uptake of label into the matrix within 20 s was only 22% of the pellet content. This can be seen in Fig. 3A from the high radioactivity in the pellet at  $t = 0$ , which was mainly due to the  $[^{14}\text{C}]\text{aspartate}$  in the sucrose-accessible space, i.e., the extra-matrix space of the pellet and, to a lesser extent (less than 13%), due to the residual uptake during the quenching time of the inhibitor (Fig. 2). These problems of method became even more severe in experiments with lower internal aspartate concentrations,

because the isotope equilibration with the small internal substrate pool is faster and, as a consequence, the initial linear phase is shorter.

From these initial rate experiments (Fig. 3), the following conclusions could be drawn: (a) the activity of the carrier at  $2^\circ\text{C}$  was relatively low with isotope equilibration occurring on a time scale of minutes (Fig. 3B); (b) the external  $K_m$  for aspartate calculated from Fig. 3A was in the range of 200–300  $\mu\text{M}$ ; and (c) the accuracy obtained in these experiments was insufficient for a bisubstrate kinetic analysis of the antiport mechanism, which requires reliable measurements of the initial rate at a sufficiently large range of substrate concentrations on both sides of the membrane. This led us to consider the full time course of  $[^{14}\text{C}]\text{aspartate}$  uptake.

#### Full progress-curve experiments

Under homoexchange conditions the substrate concentrations in both compartments remain constant. Thus, full progress-curves describing  $[^{14}\text{C}]\text{aspartate}$  uptake till equilibrium can be used to calculate the actual initial steady-state rate without any particular assumption, except that a steady-state is reached. Knowing the  $[^{14}\text{C}]\text{aspartate}$  uptake at equilibrium ( $Y_{\text{eq}}$ ), the progress-curve can be linearized according to:

$$Z = Y_{\text{eq}} \ln \frac{Y_{\text{eq}}}{Y_{\text{eq}} - Y_t} = vt \quad (1)$$

where  $Y_t$  is the uptake after incubation time  $t$  (uptake at  $t = 0$  subtracted).  $Z$  can be rationalized as the

uptake corrected for the variation (during isotope equilibration) of the external and internal specific radioactivities of aspartate. The initial rate,  $v$ , represents the velocity of unidirectional aspartate uptake (not only of label), which in fact is constant throughout the whole experiment (see below, Fig. 4). The quench delay of the inhibitor in a given time-course is a constant time that has to be added to  $t$  (Eqn. 1) and does not modify the slope. Furthermore, it is small compared with the incubation times considered.

Fig. 3B shows the progress-curves for the same mitochondrial preparation as used in Fig. 3A and for the same internal and external aspartate concentrations. Equilibrium was reached after an incubation for 30 to 60 min.  $Y_{eq}$  was  $1.25 \text{ nmol}/\mu\text{l}$  which was in good agreement with the theoretical value calculated from the external and internal substrate pools. In Fig. 3B, as in Fig. 3A, the labelled aspartate in the pellet at  $t = 0$  was not subtracted in order to show that these values were small compared with  $Y_{eq}$ , thereby demonstrating the much better signal to noise ratio compared with that for Fig. 3A.

The linearization of the progress-curves according to eqn. 1 is presented in Fig. 4, where  $Z$  was plotted vs. time. A perfect linearity was observed indicating that the progress-curves were well-fitted by a single exponential equation. Due to this methodological im-

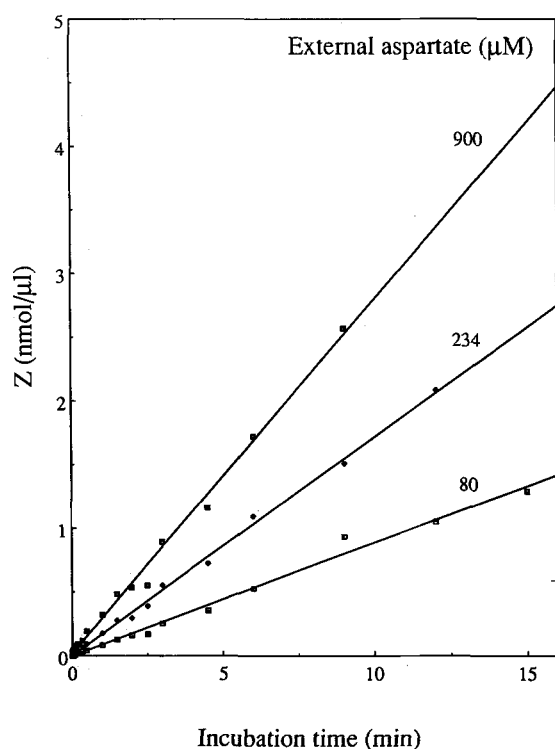


Fig. 4. Initial rate measurements from full progress-curves. The  $Z$  values (for explanation see text) were calculated from the full progress-curves of Fig. 3B. The initial rates derived from the slope of the straight lines are given in the text.

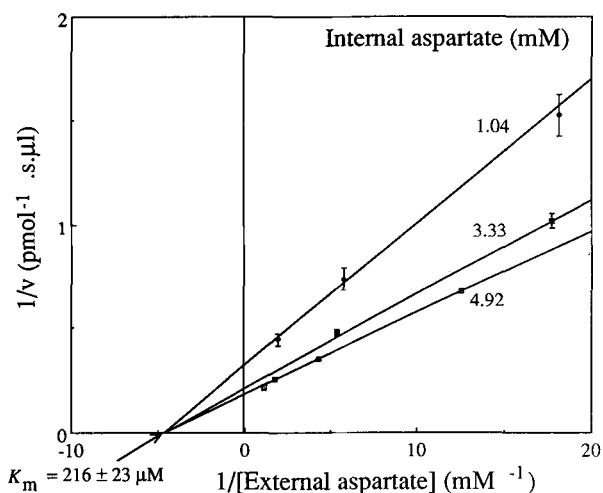


Fig. 5. Influence of the external aspartate concentration on the initial rate of  $[^{14}\text{C}]\text{aspartate}_{out}/\text{aspartate}_{in}$  exchange for three internal aspartate concentrations. Full progress-curves were recorded at different concentrations of internal and external aspartate as indicated ( $2^\circ\text{C}$ , pH 7.4). Initial rates ( $\pm \text{S.D.}$ ) were calculated from the slopes of  $Z$  vs. time (see Fig. 4). The straight lines were fitted imposing a common intersection point on the abscissa axis (unknown a priori).

provement the initial rates obtained from the slopes of Fig. 4 were much more precise ( $1.48 \pm 0.03$ ,  $2.86 \pm 0.03$ ,  $4.65 \pm 0.06 \text{ pmol/s per } \mu\text{l}$  for 80, 234 and  $900 \mu\text{M}$  external aspartate, respectively) and showed only a low standard deviation. Moreover, the number of experimental data points (26 between zero time and equilibrium) led to a high statistical weight of the initial rate values.

#### Bisubstrate kinetic analysis

In order to elucidate the transport mechanism of the aspartate/glutamate carrier we had to investigate the mutual interaction of internal and external substrate with the carrier. For this purpose the experiment described in Fig. 4, where only the external substrate was varied, was reproduced at different internal aspartate concentrations. The incubation times were adjusted to obtain proper equilibrium values ( $Y_{eq}$ ) and a valuable kinetic resolution. Three sets of initial velocity values were determined from the full progress-curves for three internal aspartate concentrations (1.04, 3.3 and 4.9 mM) which are given in the double reciprocal plots of Fig. 5. The straight lines obtained by linear regression showed convergence very close to the abscissa which indicates a sequential type of kinetic transport mechanism (see Discussion). If a common intersection point was placed on the abscissa (Fig. 5), calculations by a least square method [2] led to a  $K_m$  value of  $216 \pm 23 \mu\text{M}$  for external aspartate.

The convergence on the abscissa as observed in Fig. 5 indicated that the value of the external  $K_m$  was independent of the internal aspartate concentration and vice versa. The internal  $K_m$  could thus also be

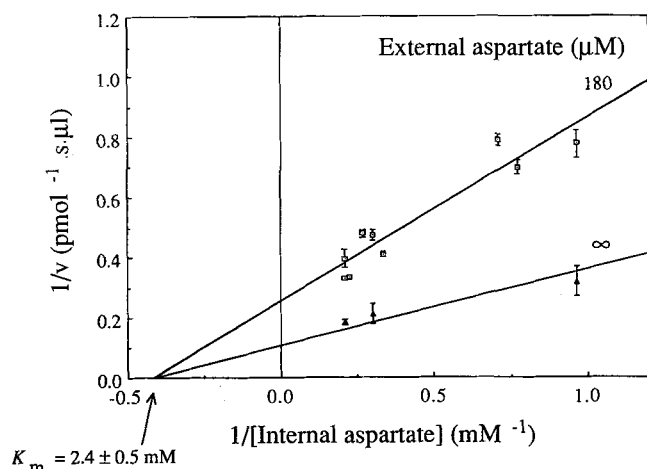


Fig. 6. Influence of the internal aspartate concentration on the initial rate of  $[^{14}\text{C}]\text{aspartate}_{\text{out}}/\text{aspartate}_{\text{in}}$  exchange for limiting and infinite external aspartate. Full progress-curves were recorded at different internal aspartate concentrations and 180  $\mu\text{M}$  external  $[^{14}\text{C}]\text{aspartate}$  ( $2^\circ\text{C}$ , pH 7.4). The data for infinite external aspartate concentration were taken from Fig. 5 ( $V_{\text{max}}$  values). The internal glutamate was less than 7% of the internal aspartate for each condition.

determined at limiting external aspartate concentrations. In the experiments of Fig. 6 initial rates were derived from full progress-curves obtained at different internal aspartate concentrations in the range of 1–5 mM with the external  $[^{14}\text{C}]\text{aspartate}$  kept constant at 180  $\mu\text{M}$ . The scattering of data points in the double reciprocal plot may be attributed to the fact that every single rate necessarily had to be determined in different mitochondrial preparations. Nevertheless, a linear relationship was obtained leading to an internal  $K_m$  of about 3 mM (not shown). The  $K_m$  for internal aspartate could also be evaluated by replotting the ordinate intercepts of Fig. 5, i.e., the reciprocal exchange velocities at infinite external aspartate, vs. (internal aspartate) $^{-1}$ . This secondary plot was included in Fig. 6. Again a common intersection point of the two straight lines was observed close to the abscissa representing a more reliable value of the internal  $K_m$  ( $2.4 \pm 0.5$  mM). The maximum exchange rate extrapolated for infinite concentration of both internal and external aspartate was  $9.4 \pm 1.6$   $\text{pmol s}^{-1} \mu\text{l}^{-1}$  which was equal to  $2.8$   $\text{nmol min}^{-1} \text{mg protein}^{-1}$ .

#### Comparison with the reconstituted system

Detailed kinetic studies of the aspartate/glutamate carrier from beef heart mitochondria have been carried out in the reconstituted system [10,13]. As observed in intact mitochondria (Fig. 5), bisubstrate kinetics led to a pattern of intersecting straight lines converging very close to the abscissa. In order to substantiate this basic agreement of results from intact mitochondria and proteoliposomes, it was considered interesting to find out whether the interaction of substrate with carrier, as

TABLE II

*Influence of pH on the  $K_m$  values of the reconstituted aspartate/glutamate carrier for external and internal aspartate*

The exchange velocity was determined by the forward exchange method measuring uptake of  $[^{14}\text{C}]\text{aspartate}$  supplied in different concentrations (external  $K_m$  determinations: 25–260  $\mu\text{M}$ , internal  $K_m$  determinations: 50  $\mu\text{M}$ ) to proteoliposomes containing 16 mM or, in the case of internal  $K_m$  determinations, 1–9 mM aspartate. The  $K_m$  values were derived from reciprocal plots (Lineweaver-Burk and Eadie-Hofstee) and are given as mean values from four determinations. For adjustment of pH see Materials and Methods.

pH	External $K_m$ (mM)	Internal $K_m$ (mM)
6.5	$0.044 \pm 0.003$	$2.6 \pm 0.3$
6.9	$0.084 \pm 0.008$	$3.7 \pm 0.6$
7.4	$0.123 \pm 0.011$	$2.8 \pm 0.6$

characterized by internal and external  $K_m$  values, was quantitatively comparable in the two systems. It had already been shown [13] that the affinity of the reconstituted aspartate/glutamate carrier for aspartate is much higher on the outside of the proteoliposomes ( $K_m$ : 50  $\mu\text{M}$ ) than on the inside ( $K_m$ : 3 mM). These  $K_m$  values were obviously affected by the pH [10], which was 7.4 in the experiments presented above but 6.5 in the studies using proteoliposomes. Therefore, the affinity of the reconstituted aspartate/glutamate carrier for aspartate was redetermined on both sides of the liposomal membrane raising the pH from 6.5 to 7.4. In order to avoid difficulties resulting from pH gradients, the pH was adjusted in parallel in both compartments (see Materials and Methods). As demonstrated in Table II, a clear increase in  $K_m$  with the pH from 44 (pH 6.5) to 123  $\mu\text{M}$  (pH 7.4) was observed at the external side, whereas the internal values calculated at pH 6.5, 6.9 and 7.4 were all in the range of 3 mM. Consequently, at pH 7.4 a close correlation with the transport affinities determined in intact rat heart mitochondria became evident although the species of mammal differed.

#### Discussion

Two basic aspects appeared to be important when reinvestigating the kinetic properties of the aspartate/glutamate carrier in intact mitochondria. Firstly, to clarify the controversy over results obtained more than 10 years ago concerning the kinetic mechanism of the carrier in intact mitochondria [6] and in submitochondrial particles [5]. Secondly, to elucidate from comparative studies carried out in intact mitochondria and in the reconstituted system how these two analytic systems can supplement and reinforce each other. If so, this new approach would enable the results obtained from kinetic experiments in liposomes and in mitochondria to be combined in order to draw conclu-

TABLE III

*Michaelis constants for aspartate of the mitochondrial aspartate / glutamate carrier at pH 7.4*

System	Temperature (°C)	$K_m$ for aspartate (mM)	
		matrix side	cytosolic side
Intact rat-heart mitochondria (this paper)	2	$2.4 \pm 0.5$	$0.216 \pm 0.023$
Proteoliposomes, carrier from bovine-heart mitochondria (this paper)	Room temperature	$2.8 \pm 0.6$	$0.123 \pm 0.011$
Inverted rat-heart submitochondrial particles [5]	17	0.042	—
Intact rat-liver mitochondria (pH 7.2) [6]	10	5.0	—

sions that are meaningful for the *in vivo* situation of the carrier.

#### *The kinetic mechanism*

The usefulness of the kinetic approach for studying mechanisms of mitochondrial translocators is often limited by technical problems; in fact initial rates may be difficult to obtain. It is thus important to carry out direct and careful kinetic measurements and, if possible, to apply different experimental systems. The kinetic mechanism of the mitochondrial aspartate/ glutamate carrier analyzed here in intact rat heart mitochondria is in complete accord with that observed in the reconstituted system [10]. Moreover, the measured  $K_m$  values on both sides of the membrane show striking numerical coincidence (see Table III), although the aspartate/ glutamate carrier from different sources was investigated, i.e., from rat and bovine heart, respectively. Such a comparison has been made for the first time and provides strong evidence that this translocator does not follow a ping-pong mechanism but a sequential one, as shown in double reciprocal plots by the presence of intersecting straight lines converging near the abscissa. This type of kinetic pattern indicates that considerably raising the substrate concentration in one compartment increases the transport rate ( $V_{max}$ ) without much effect on the affinity of the carrier for the substrate in the opposite compartment. On the contrary, in a ping-pong mechanism both  $V_{max}$  and  $K_m$  are affected to the same degree leading to parallel straight lines in the double reciprocal plots. Consequently, for the sequential mechanism, the association of internal and external substrate with the carrier cannot be separated by translocation steps. This means that one internal and one external binding site of the carrier protein must be occupied forming a transport-competent ternary complex. The position of the common intersection point on the abscissa suggests that the binding of the internal and the external substrate is fast and independent (rapid-equilibrium random).

Previous publications on the kinetic mechanism of the mitochondrial aspartate/ glutamate carrier [5,6] (for review see Ref. 13) give conflicting results. The signifi-

cant methodological improvements for correct evaluation of initial exchange rates presented in this paper enabled these to be resolved, at least for studies using intact mitochondria. On the one hand, data previously obtained for submitochondrial particles from rat heart mitochondria could be rejected. Although insufficiently precise, these were interpreted to be consistent with a ping-pong mechanism [5]. On the other hand, the kinetic pattern reported here agrees, in principle, with that obtained for intact rat liver mitochondria [6].

In view of the existence of a so-called 'protein super-family' of mitochondrial carriers it is important to find out whether its members can be characterized in terms of a common kinetic mechanism as well as by their structural similarities [22,23]. The sequential mechanism involving two substrate binding sites, one on each membrane side (see above), was also elucidated for the oxoglutarate carrier in early investigations carried out in rat heart mitochondria [1–4]. More precisely, the mechanism of the oxoglutarate carrier could be described as a rapid-equilibrium random mechanism with fast and independent binding of one internal and one external substrate molecule. These results were convincingly confirmed for the reconstituted carrier from beef heart (Indiveri, C., Dierks, T., Krämer, R. and Palmieri, F., unpublished data). As shown here, this particular mechanism also holds true for the aspartate/ glutamate carrier. It should be noted that the transport mechanism of the ADP/ATP carrier, the most intensively studied mitochondrial carrier, was described as a gated pore mechanism involving a single binding center [24,25], which in kinetic terms would be classified as a ping-pong mechanism. This model was mainly based on studies measuring the accessibility of binding sites in the two different conformational states of the carrier which can be trapped by side-specific inhibitors. However, binding studies also led to alternative models involving at least one binding site on either membrane side ([26] and references therein). Kinetic investigations of the exchange reaction also provided direct evidence for a sequential mechanism [7–9]. Thus, a general concept seems to evolve of a functional carrier family, so far consisting of three of the main mitochondrial antiporters, namely

the oxoglutarate, the aspartate/glutamate and the ADP/ATP carriers.

#### *The orientation of the carrier in the reconstituted system*

As determined in the present paper for both intact mitochondria and proteoliposomes, the external binding site of the aspartate/glutamate carrier showed a significantly lower  $K_m$  for aspartate (0.22 and 0.12 mM, respectively) than the internal site (2.4 and 2.8 mM, respectively) (Table III). This correlation clearly indicates a right-side out orientation of the reconstituted protein. The excellent agreement suggests that the  $K_m$  values derived from transport studies are similar for the carrier protein from different organisms and are unaffected by isolation or by the different temperatures applied in the experiments (Table III). The influence of pH on  $K_m$  values was taken into account (Table II), thereby improving the reliability of this comparison. It appears that internal  $K_m$  for aspartate is at least one order of magnitude higher than the external  $K_m$ . Such an asymmetry has been already observed with the oxoglutarate carrier of rat-heart mitochondria for oxoglutarate [3,9]: close to 2 orders of magnitude.

The observed right-side out transmembrane topology in proteoliposomes is in contrast to the previous interpretation of an inside out orientation of the reconstituted carrier protein [13]. This conclusion was based mainly on the matrix  $K_m$  value for aspartate (0.042 mM) found by LaNoue and co-workers [5] on the outside of inverted submitochondrial particles (Table III). However, in this study the degree of inversion of the particles was not indicated. Other  $K_m$  (or  $K_i$ ) values reported for aspartate, sometimes based on indirect methods, were all in the range of 3–5 mM on both the matrix (Table III) and the cytosolic side, as discussed in [13]. Hence, they could not be used to confirm the correct definition of the orientation of the reconstituted protein. This definition was only made possible by the results of the present paper giving the  $K_m$  values for the same substrate (aspartate) on the two different sides of the membrane for both the native and the reconstituted systems, thereby demonstrating the strength of comparative kinetic studies of this type. It should be pointed out that the matrix  $K_m$  for aspartate (5.0 mM) and the cytosolic  $K_m$  for glutamate at high pH (5.8 mM) found by Murphy et al. [6] in liver mitochondria was of the same order of magnitude as our data (2.8 mM and 1.8 mM, Table III and [10], respectively).

The evaluation of this right-side out transmembrane arrangement of the carrier in proteoliposomes is of importance for further studies of the malate-aspartate shuttle reconstituted in liposomes. It is also of interest in relation to the recent observation of unidirectional export activity of the reconstituted aspartate/glutamate carrier induced by cysteine-modifying

reagents [21,27]. According to the 'physiological' transmembrane orientation of the reconstituted carrier, this function can be related to the efflux phenomena generally observed in mitochondria after treatment with SH-reagents.

#### **Acknowledgements**

Our thanks are due to Eli Dethier for his skilful technical assistance. This work was supported by grants from the Belgian 'Fonds National de la Recherche Scientifique', the 'Fonds Special de la Recherche dans les Universités', the 'Fonds de Recherche de la Faculté de Médecine', the 'Deutsche Forschungsgemeinschaft' (SFB 189) and the 'Fonds der Chemischen Industrie'. A.E. is a fellow of I.R.S.I.A.

#### **References**

- Sluse, F.E., Ranson, M. and Liébecq, C. (1972) *Eur. J. Biochem.* 25, 207–217.
- Sluse, F.E., Goffart, G. and Liébecq, C. (1973) *Eur. J. Biochem.* 32, 283–291.
- Sluse-Goffart, C.M., Sluse, F.E., Duyckaerts, C., Richard, M., Hengesch, P. and Liébecq, C. (1983) *Eur. J. Biochem.* 134, 397–406.
- Sluse-Goffart, C.M. and Sluse, F.E. (1986) in *Dynamics of Biochemical Systems* (Damjanovich, S., Keleti, T. and Tron, L., eds.), pp. 521–535, Elsevier, Amsterdam.
- LaNoue, K.F., Duszynski, J., Watts, J.A. and McKee, E. (1979) *Arch. Biochem. Biophys.* 195, 578–590.
- Murphy, E., Coll, K.E., Viale, R.O., Tischler, M.E. and Williamson, J.R. (1979) *J. Biol. Chem.* 254, 8369–8376.
- Duyckaerts, C., Sluse-Goffart, C.M., Fux, J.P., Sluse, F.E. and Liébecq, C. (1983) *Eur. J. Biochem.* 134, 397–406.
- Barbour, R.L. and Chan, S.H.P. (1981) *J. Biol. Chem.* 256, 1940–1948.
- Sluse, F.E., Sluse-Goffart, C.M. and Duyckaerts, C. (1989) in *Anion Carriers of Mitochondrial Membranes* (Azzi, A., Nalecz, K.A., Nalecz, M.J. and Wojtczak, L., eds.), pp. 183–195, Springer Verlag, Berlin.
- Dierks, T., Riemer, E. and Krämer, R. (1988) *Biochim. Biophys. Acta*, 943, 231–244.
- Krämer, R. and Heberger, C. (1986) *Biochim. Biophys. Acta*, 863, 289–296.
- Krämer, R., Kürzinger, G. and Heberger, C. (1986) *Arch. Biochem. Biophys.* 251, 166–174.
- Dierks, T. and Krämer, R. (1988) *Biochim. Biophys. Acta*, 937, 112–126.
- Duyckaerts, C., Sluse-Goffart, C.M., Evens, A., Camus, G., Dierks, T., Krämer, R. and Sluse, F.E. (1989) *Abstr. Int. Symp. on 'Structure, Function and Bioenergetics of Energy Transfer Systems'*, Bari, p. T29.
- Evens, A., Duyckaerts, C., Sluse-Goffart, C.M., Dierks, T., Krämer, R. and Sluse, F.E. (1990) *Arch. Int. Physiol. Biochim.* 98, B70.
- Evens, A., Duyckaerts, C., Sluse-Goffart, C.M., Dierks, T., Krämer, R. and Sluse, F.E. (1990) *Abstr. 6th Eur. Bioenerg. Conf.*, Noordwijkerhout, p. 36.
- Tyler, D.D. and Gonze, J. (1967) *Methods Enzymol.* 10, 75–77.
- Sluse, F.E., Duyckaerts, C., Liébecq, C. and Sluse-Goffart, C.M. (1979) *Eur. J. Biochem.* 100, 3–17.
- Jones, B.N. and Gilligan, J.P. (1983) *J. Chromatogr.* 266, 471–482.

- 20 Klingenberg, M. and Pfaff, E. (1967) *Methods Enzymol.* 10, 680–684.
- 21 Dierks, T., Salentin, A., Heberger, C. and Krämer, R. (1990) *Biochim. Biophys. Acta*, 1028, 268–280.
- 22 Aquila, H., Link, T.A. and Klingenberg, M. (1987) *FEBS Lett.* 212, 1–9.
- 23 Runswick, M.J., Powell, S.J., Nyren, P. and Walker, J.E. (1987) *EMBO J.* 6, 1367–1373.
- 24 Klingenberg, M. (1989) *Arch. Biochem. Biophys.* 270, 1–14.
- 25 Klingenberg, M. (1981) *Nature* 290, 449–454.
- 26 Block, M.C. and Vignais, P.V. (1984) *Biochim. Biophys. Acta* 767, 369–376.
- 27 Dierks, T., Salentin, A. and Krämer, R. (1990) *Biochim. Biophys. Acta* 1028, 281–288.